Ferroelectrics, 463:1–7, 2014

ISSN: 0015-0193 print / 1563-5112 online
DOI: 10.1080/00150193.2014.891416

Taylor & Francis
Taylor & Francis Group

Giant LO-TO Frequency Splitting of the Soft Mode in Perovskites

G. KOMANDIN, O. PORODINKOV,* I. SPEKTOR, S. CHUCHUPAL, AND A. VOLKOV

A. M. Prokhorov General Physics Institute, Russian Academy of Sciences, Moscow, Russia

The dispersion analysis of the dielectric spectra of the perovskite ceramics, $CaTiO_3$, and perovskite-like monocrystalline thin films $(Ba,Sr)TiO_3$ deposited on a monocrystalline MgO substrate is carried out. The giant LO–TO splitting ($\sim$700 cm^{-1}) of the lowest-frequency absorption band (the soft mode) is found. Due to that splitting the LO and TO frequencies of other phonons are inverted. The result is in a good agreement with first-principle calculations.

Keywords Ferroelectric; perovskite; permittivity; LO–TO splitting; dispersion analysis

Introduction

Calcium titanate, $CaTiO_3$, is the forefather of the structural family of perovskite (a general formula of perovskites is ABO_3, where A and B – the metal atoms). Despite that the calcium titanate is a paraelectric under the ambient conditions, it is an object of many investigations on ferroelectricity, in particular, by methods of the IR and the Raman spectroscopy [1–3]. The simplicity of the structure makes crystal ABO_3 systems convenient to perform both experimental and theoretical studies on the lattice dynamics, physics of structural phase transitions, ferroelectric-related phenomena.

In departure of the $CaTiO_3$, barium titanate and solid solutions $(Ba,Sr)TiO_3$ (BST) with high content of Ba are ferroelectrics. They possess high permittivity at small dielectric losses and leakage currents; in addition, they are weakly subjected to fatigue and aging. Therefore, their electrodynamic characteristics are under active study to apply these materials in microelectronics [4–6]. Especially promising are the multilayer film structures. Structures are synthesized via film deposition on a substrate at temperatures of several hundreds of degrees. During cooling, mechanical stresses arise in the films due to the lattice mismatch and difference in thermal expansion coefficients of the film and the substrate, as well as because of spontaneous polarization in the film after the deposition. The stresses form the phase states in films, which are not commonly realized in bulk crystals and ceramics [7, 8].

The perovskites are characterized by a large Born dynamical effective charge of the soft mode and the low soft mode frequency ($<$100 cm^{-1}) which results in the high value

Received September 2, 2013; in final form October 4, 2013.
*Corresponding author. E-mail: oporodinkov@ran.gpi.ru
Color versions of one or more of the figures in the article can be found online at www.tandfonline.com/gfer.

of the dielectric constant. Due to that, a common electrodynamic feature is inherent in perovskites caused by the long-range Coulomb interactions [9], namely, an anomalously large frequency splitting of the longitudinal ν_{LO} and transverse ν_{TO} optical phonons:

$$\nu_{LO}^2 - \nu_{TO}^2 = \frac{4\pi e_B^2}{V\mu}, \tag{1}$$

where e_{B} is the Born charge, V is the unit cell volume, and μ is the reduced dipole mass. The larger the effective charge of the mode, the larger the LO–TO splitting and, correspondingly, its dielectric contribution:

$$\Delta\varepsilon_j = \varepsilon_\infty \frac{\nu_{jLO}^2 - \nu_{jTO}^2}{\nu_{jTO}^2} \prod_{k\neq j} \frac{\nu_{kLO}^2 - \nu_{jTO}^2}{\nu_{kTO}^2 - \nu_{jTO}^2}. \tag{2}$$

First-principle calculations [9] predict giant LO–TO splitting of the soft mode for perovskites giving, in particular, ~700 cm^{-1}, ~550 cm^{-1} and ~770 cm^{-1} for cubic calcium titanate, barium titanate and strontium titanate, respectively. The goal of our study is to establish the direct pair relations between the TO and LO modes in the model $CaTiO_3$ and BST/MgO samples by the analysis of their panoramic reflection spectra.

Experimental Results and Discussion

The starting data for the analysis were the reflection and transmission spectra of the $CaTiO_3$ ceramics (Fig. 1) and the structures $Ba_{0.8}Sr_{0.2}TiO_3$/MgO (Fig. 2) measured at room temperature with the use of IR Fourier spectrometer Bruker-113v in the 20–4000 cm^{-1} range and a backward wave oscillator (BWO) spectrometer [10] in the 4–20 cm^{-1} range.

The dispersion analysis was performed with the use of two models: three-parametric additive model of the Lorentz harmonic oscillators and Lyddane-Sachs-Teller factorized four-parametric model [11]. First, the spectra of the real $\varepsilon'(\nu)$ and imaginary $\varepsilon''(\nu)$ parts of permittivity were treated by the Lorentzians:

$$\varepsilon'(\nu) = \varepsilon_\infty + \sum_{j=1}^{n} \frac{\Delta\varepsilon_j \nu_j^2 \left(\nu_j^2 - \nu^2\right)}{\left(\nu_j^2 - \nu^2\right)^2 + \gamma_j^2 \nu^2}, \tag{3}$$

$$\varepsilon''(\nu) = \sum_{j=1}^{n} \frac{\Delta\varepsilon_j \nu_j^2 \nu\gamma_j}{\left(\nu_j^2 - \nu^2\right)^2 + \gamma_j^2 \nu^2}, \tag{4}$$

where ν_{j} is the eigenfrequency, γ_{j} is damping, and $\Delta\varepsilon_{\mathrm{j}}$ is the dielectric contribution of the j-th transverse optical phonon.

Frequencies of longitudinal modes, LO, are not present in expressions (3, 4) in the explicit form. However, ν_{LO} can be found by the following way. Starting from the $\varepsilon'(\nu)$ and $\varepsilon''(\nu)$ spectra one can calculate the spectrum $\mathrm{Im}[1/\varepsilon^*(\nu)]$. In the case of weak anharmonicity, frequency maxima of the $\varepsilon''(\nu)$ spectra are close to the frequencies ν_{TO} of TO phonons and correspond to the poles of the dielectric response function $\varepsilon^*(\nu)$. Then, the maxima of $\mathrm{Im}[1/\varepsilon^*(\nu)]$ spectrum correspond to the zeros of the $\varepsilon^*(\nu)$ and, correspondingly, their frequencies are close to the frequencies of longitudinal optical phonons ν_{LO}:

$$\mathrm{Im}\left(\frac{1}{\varepsilon^*(\nu)}\right) = \frac{\Delta\varepsilon}{\varepsilon_0\varepsilon_\infty} \frac{\nu_{LO}^2 \gamma_{TO} \nu}{(\nu_{LO}^2 - \nu^2)^2 + \gamma_{TO}^2 \nu^2}, \tag{5}$$

where ε_0 is the static dielectric constant.

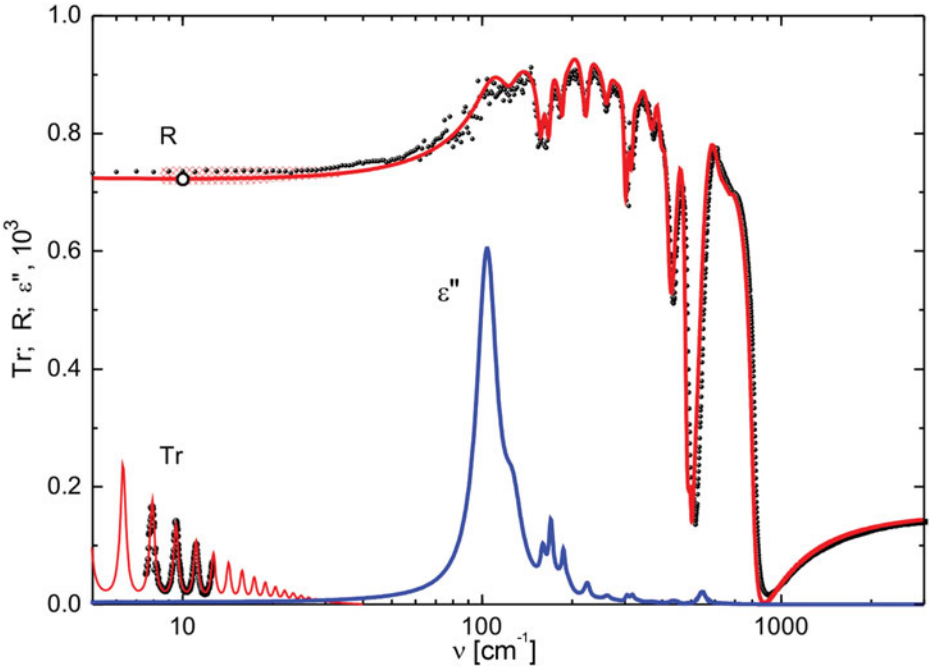

Figure 1. Experimental (points) and model (lines) reflection R(ν), transmission Tr(ν) and absorption $\varepsilon''(\nu)$ spectra of the orthorhombic $CaTiO_3$. Circle is a reference value for R calculated from the Tr(ν) spectrum.

Noteworthy, the spectra $\varepsilon''(\nu)$ and Im[$1/\varepsilon^*(\nu)$] show only the frequency location of the transverse and longitudinal vibrations, but they do not give mutual correspondence of the TO and LO modes. This does not allow to identify the magnitude of the LO–TO splitting. Otherwise, the interrelation between the LO and TO modes is established by four-parametric dispersion model [11]:

$$\varepsilon*(\nu) = \varepsilon_\infty \prod_j \frac{\nu_{jLO}^2 - \nu^2 + i\nu\gamma_{jLO}}{\nu_{jTO}^2 - \nu^2 + i\nu\gamma_{jTO}}. \tag{6}$$

We fitted the model (6) to the experimental $\varepsilon'(\nu)$ and $\varepsilon''(\nu)$ spectra with the parameters $\Delta\varepsilon_j$ and ν_{jTO} of the previous model (3, 4). The dispersion parameters for the orthorhombic calcium titanate are presented in Table 1. The uncertainties are estimated as 10 % for $\Delta\varepsilon$ and γ, and 5 % for ν.

For simplicity, Table 1 shows the parameters of the first five oscillators with dominating dielectric contribution. Parameters of the first mode reveal a relaxation character of the low-frequency response: $\gamma_{1TO} = 40\ \mathrm{cm}^{-1} > \nu_{1TO} = 15\ \mathrm{cm}^{-1}$. This relaxation is associated with the morphology of the sample since its parameters depend on the structure of the ceramics [11–13]. The other oscillators represent the phonon spectrum of $CaTiO_3$. A complete set of oscillators and their analysis is given in [14, 15]. Correspondent graphs are shown in Fig. 3.

Table 1
The dispersion parameters of the orthorhombic $CaTiO_3$, $\varepsilon_\infty = 5.3$

N	ν_{TO} [cm^{-1}]	γ_{TO} [cm^{-1}]	ν_{LO} [cm^{-1}]	γ_{LO} [cm^{-1}]	$\Delta\varepsilon$
L1 Relax	15	40	15	40	5
L2	104	19	805	39	109
L3	*127*	21	*122*	21	18
L4	*159*	7	*157*	8	2
L5	*170*	6	*167*	8	2
...	...	...	...	...	...

Figure 3 illustrates a giant (~700 cm^{-1}) splitting of the longitudinal and transverse frequencies of the soft mode (L2 oscillator in Table 1), which extends between the low-frequency maximum of $\varepsilon''(\nu)$ and the high-frequency maximum of Im$[1/\varepsilon^*(\nu)]$. All IR-active vibrations fill up the region of negative values of ε', i.e., are into the region of the LO–TO splitting of the soft mode. As a consequence, frequencies of longitudinal and transverse components of these vibrations are inverted (the frequencies of inverted phonons L3–L5 in Table 1 are italicized). This result agrees wholly with what is reasoned in Ref. [9] based on first-principle calculations.

Our measurement of the dielectric spectra of thin ferroelectric films on a dielectric substrate is described in detail in [16–18]. The dispersion parameters of the 1.5 mkm

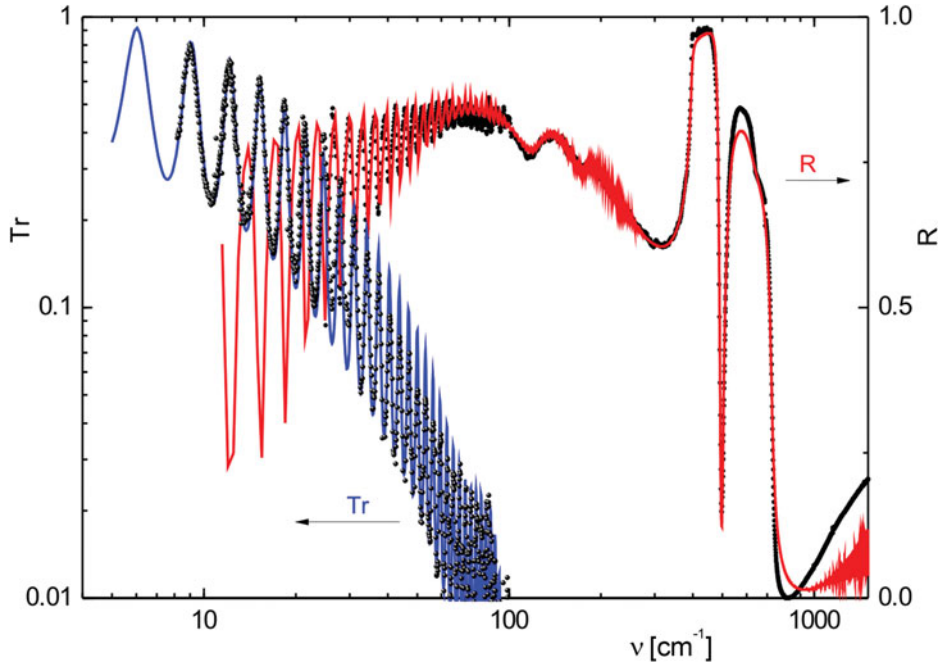

Figure 2. Experimental (points) and model (lines) reflection R(ν) and transmission Tr(ν) spectra of the BST/MgO structure. Low-frequency part of the reflection spectrum R(ν) is calculated from the transmission spectrum Tr(ν).

Table 2
The dispersion parameters of the 1.5 mkm BST film, $\varepsilon_\infty = 4.5$

N	ν_{TO} [cm^{-1}]	γ_{TO} [cm^{-1}]	ν_{LO} [cm^{-1}]	γ_{LO} [cm^{-1}]	$\Delta\varepsilon$
L1	46	50	738	49	380
L2	*65*	41	*56*	46	226
L3	*130*	28	*124*	30	13
L4	*178*	20	*176*	20	1.4
L5	*511*	16	*472*	15	0.7

$Ba_{0.8}Sr_{0.2}TiO_3$/MgO film are presented in Table 2. The corresponding illustrative graphs are shown in Fig. 4.

Similar to that occurring in $CaTiO_3$, the giant LO–TO splitting of the soft mode (L1 oscillator in Table 2), as well as a frequency inversion of the other TO and LO phonons (L2–L5) take place (frequencies of inverted phonons in Table 2 are italicized).

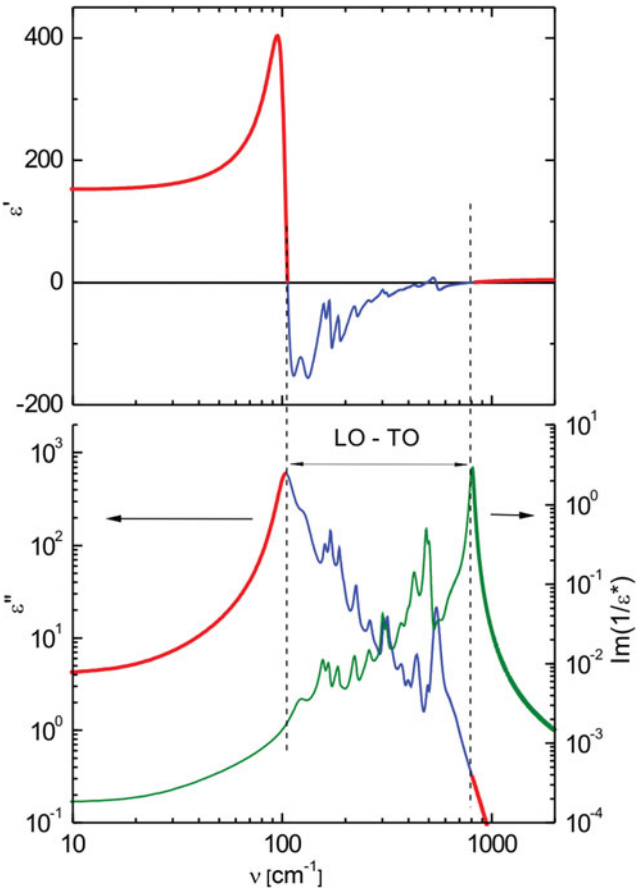

Figure 3. Frequency panorama of the TO and LO phonons for orthorhombic $CaTiO_3$ in terms of the $\varepsilon'(\nu)$ and $\varepsilon''(\nu)$ spectra and dielectric loss function Im$[1/\varepsilon^*(\nu)]$.

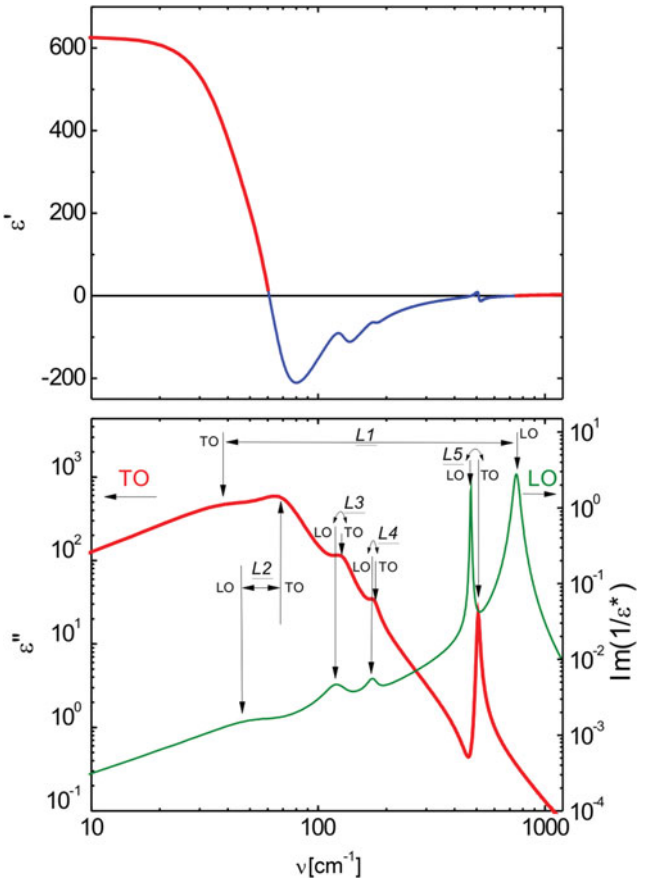

Figure 4. Frequency panorama of the TO and LO phonons for the BST film (1500 nm) in the BST/MgO structure in terms of the $\varepsilon'(\nu)$ and $\varepsilon''(\nu)$ spectra and the dielectric loss function $\mathrm{Im}[1/\varepsilon^*(\nu)]$.

Conclusion

The dispersion analysis of the panorama has been performed in the frameworks of two dispersion models, additive and factorized. The correspondence of longitudinal and transverse IR-active vibrations has been established for the cubic and orthorhombic phases. Giant LO–TO splitting (700 cm^{-1}) of the low frequency soft mode has been found which led to frequency inversion of all IR vibrations falling to this region. This result is in good agreement with first principle calculations.

References

1. A. Linz and K. Herrington, Electrical and optical properties of synthetic calcium titanate crystal. *J Chem Phys.* **28**, 824–825 (1958).
2. C. H. Perry, B. N. Khanna, and G. Rupprecht, Infrared studies of perovskite titanates. *Phys Rev.* **135**, 408–412 (1964).
3. G. Rupprecht and R. O. Bell, Dielectric constant in paraelectric perovskites. *Phys Rev.* **135**, 748–752 (1964).
4. J. F. Scott, Applications of Modern Ferroelectrics. *Science.* **315**, 954–959 (2007).

5. A. S. Sigov, E. D. Mishina, and V. M. Mukhortov, Thin ferroelectric films: Preparation and prospects of integration. *Phys Solid State.* **52**, 762–770 (2010).
6. N. Setter, D. Damjanovic, L. Eng, G. Fox, S. Gevorgian, S. Hong, A. Kingon, H. Kohlstedt, N. Y. Park, G. B. Stephenson, I. Stolichnov, A. K. Taganstev, D. V. Taylor, T. Yamada, and S. Streiffer, Ferroelectric thin films: Review of materials, properties, and applications. *J Appl Phys.* **100**, 051606 (2006).
7. G. A. Komandin, A. A. Volkov, I. E. Spektor, K. A. Vorotilov, and V. M. Mukhortov, Terahertz dielectric spectra of (Ba,Sr)TiO_3 thin films. *Phys Solid State.* **51**, 1351–1355 (2009).
8. Yu. I. Yuzyuk, J. L. Sauvajol, P. Simon, V. L. Lorman, V. A. Alyoshin, I. N. Zakharchenko, and E. V. Sviridov, Phase transitions in $(Ba_{0.7}Sr_{0.3})TiO_3$/MgO thin film studied by Raman scattering. *J Appl Phys.* **93**, 9930–9937 (2003).
9. W. Zhong, R. D. King-Smith, and D. Vanderbilt, Giant LO–TO splitting in perovskite ferroelectrics. *Phys Rev Lett.* **72**, 3618–3621 (1994).
10. G. V. Kozlov and A. A. Volkov, Coherent Source Submillimeter Wave Spectroscopy. *Topics in Appl Phys.* **74**, 51–109 (1998).
11. R. H. Lyddane, R. G. Sachs, and E. Teller, On the polar vibrations of alkali halides. *Phys Rev.* **59**, 673–676 (1941).
12. F. Gervais, *High-Temperature infrared reflectivity spectroscopy by scanning interferometry. In: Button KJ, eds. Infrared and millimeter waves*. New York: Academic press, 8, 279–339 1983.
13. A. S. Barker and J. J. Hopfield, Coupled-optical-phonon-mode theory in the infrared dispersion in $BaTiO_3$, $SrTiO_3$, and $KTaO_3$. *Phys Rev.* **135**, 1732–1737 (1964).
14. V. Železnỳ, E. Cockayne, J. Petzelt, M. F. Limonov, D. E. Usvyat, V. V. Lemanov, and A. A. Volkov, Temperature dependence of infrared-active phonons in $CaTiO_3$: A combined spectroscopic and first principles study. *Phys Rev B.* **66**, 224303–224337 (2002).
15. G. A. Komandin, A. A. Volkov, O. E. Porodinkov, I. E. Spektor, and S. V. Chuchupal, On the problem of the LO-TO splitting of the soft mode in $CaTiO_3$. *Phys Solid State.* **55**, 1236–1241 (2013).
16. G. A. Komandin, V. I. Torgashev, A. A. Volkov, O. E. Porodinkov, I. E. Spektor, and V. M. Mukhortov, Dielectric spectra of $Bi_{0.98}Nd_{0.02}FeO_3$ multiferroic thin films in the terahertz frequency range. *Phys Solid State.* **52**, 1842–1849 (2010).
17. G. A. Komandin, O. E. Porodinkov, I. E. Spector, and A. A. Volkov, Multiphonon absorption in a MgO single crystal in the terahertz range. *Phys Solid State.* **51**, 2045–2050 (2009).
18. G. A. Komandin, V. M. Mukhortov, O. E. Porodinkov, and I. E. Spektor, Dielectric response of (Ba,Sr)TiO_3 thin films in a terahertz and IR ranges. *Phys Solid State.* **55**, 288–292 (2013).